ISSN 0005–1144

Alenka Hren, Miro Milanovič

Dynamic Analysis of SEPIC Converter

UDK 621.314.1:004.942
IFAC 5.5.4.

Original scientific paper

In this paper a dynamic analysis of the nonisolated and isolated dc-dc SEPIC (**S**ingle **E**nded **P**rimary **I**nductance **C**onverter) based on the substitution of the switches (transistor and diode) by PWM averaged switch model equivalent circuit is presented.

The SEPIC converter is used when the wide range of input voltages is required. Besides the switches the SEPIC converter circuit consists of two inductors and two capacitors. Due to this, its dynamic model is of the fourth order differential equations system. The duty cycle and transformer turn ratio have great impact on the converter dynamics. The system parameters design guidelines are given to assure that the dynamic system has well separated resonance frequencies. The derived dynamic model was verified by simulation toolbox SimPowerSystems.

Key words: SEPIC converter, dynamic analysis, averaged switch model

1 INTRODUCTION

Computers and telecom equipment are steadily becoming more complex, providing ever higher levels of performance. Integral part of all this equipment is a dc-dc power conversion system which converts the incoming unregulated power from utility or other source, to the multiple regulated voltages required by the equipment. Nowadays, the power subsystem constitutes a significant part of the equipment cost and volume.

Such dc-dc power conversion subsystems can be realized by different circuit topologies. Among them the buck, boost, buck-boost and Cuk converters are the basic and the most used. Each of the circuit topology has its advantages and disadvantages and the choice depends on requirements for power conversion system. In general, circuits with the switch referenced to the ground node are preferred to simplify the switch driving circuits. Additionally, the non-pulsating input current is desirable to minimize EMI and reduce the need for additional filter elements. Significant advantage of the power conversion system is also the ability to generate output voltage either above or below the input voltage.

The SEPIC converter topology is one that fulfils all above requirements without inverting voltage polarity. The circuit was first developed at AT&T Bell laboratories [1] in the mid 1970s and has not been very widely used until recently. Now it is becoming more and more popular, especially in power conversion systems where the input voltage varies in wide range.

In typical dc-dc power conversion system the output voltage must be kept constant regardless of changes in the input voltage or in effective load resistance. Therefore, such system invariably requires feedback control loop. Its design is based on the dynamic model of dc-dc power conversion system. The SEPIC converter belongs to the class of the switching converters and therefore should be regarded as a nonlinear structure. In literature many different approaches for modelling such nonlinear structure are described. A current injected approach, circuit averaging and state space averaging method [2, 3, 4, 5] are the most popular. By all, the averaging and the small-signal linearization are the key steps in modelling switching converter. The state space averaging method that is described in [2] is appropriate for the modelling of switching converters operating in continuous conduction mode while is less suitable for switching converters operating in discontinuous conduction mode. The current injected method [3, 4] can be applied for switching converters operating in either continuous or discontinuous conduction mode. It is well established for modelling the basic

converters structures as are buck, boost or buck-boost. The circuit averaging method [5] was developed before the state-space averaging and due to its generality has gained a lot of interest recently.

In this paper a full order dynamic model of the SEPIC converter is derived by the method of circuit averaging and averaged switch modelling [6]. The derived dynamic model enables insight into the physical properties of the converter and gives relations between converter parameters and dynamic properties of the system. Therefore it is a good starting point in converter design-oriented analysis and also enables the design of the feedback control loop.

2 CIRCUIT AVERAGING AND AVERAGED SWITCH MODELING FOR NONISOLATED SEPIC CONVERTER

With circuit averaging method we average the converter waveforms directly rather than average the state-space equations. In this way the method gives a more physical interpretation to the model and can be applied directly to a number of different structures of converters and switch elements. The key step consists in the replacement of the converter switches with the voltage and current sources to obtain a time-invariant circuit topology. The voltage and current generators waveforms are defined to be identical to the original converter switch waveforms. For obtained time-invariant circuit the converter waveforms are averaged over one switching period to eliminate the switching harmonics.

In Figure 1 the circuit topology of the nonisolated SEPIC converter is presented. It consists of two inductances, two capacitors, one MOSFET transistor, one diode, the input voltage source and the load resistance at the output of the converter.

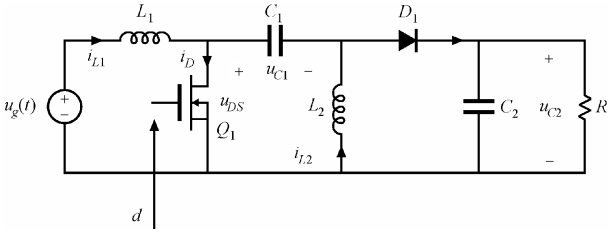

Fig. 1 The nonisolated SEPIC converter circuit topology

The basic idea of the averaged switch modelling is to find an averaged circuit model for the switch network. Then the averaged switch model is inserted into the converter circuit topology to obtain the averaged circuit model of the converter.

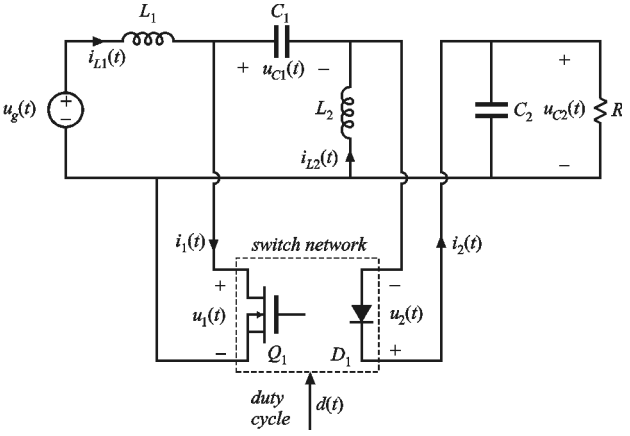

Fig. 2 Rearranged nonisolated SEPIC converter circuit topology

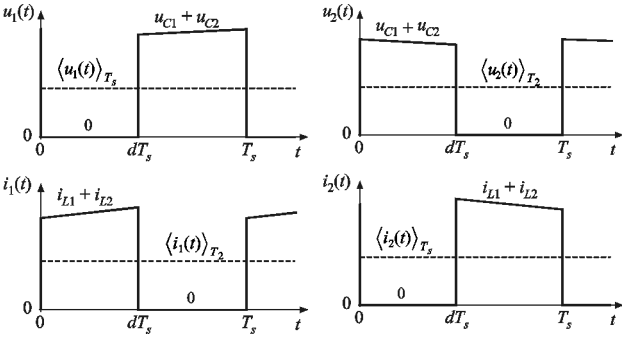

Fig. 3 The switch network terminal waveforms

The first step to obtain the averaged switch model is to sketch the converter in the form of Figure 2, where the switching elements (transistor and diode) are separated from the rest of the circuit. In Figure 3 the waveforms of the switch network of the SEPIC converter operating in continuous conduction mode are shown.

By assumption that the natural time constants of the converter are much longer than the switching time period T_S we can average the waveforms over the switching period T_S. The obtained averaged model predicts the behaviour of the system at the low frequencies and neglects the high frequency switching harmonics. The averaged values of the SEPIC switch terminal waveforms are described by:

$$\begin{aligned}
\langle u_1(t)\rangle|_{T_s} &= [1-d(t)]\left[\langle u_{C1}(t)\rangle|_{T_s} + \langle u_{C2}(t)\rangle|_{T_s}\right] \\
\langle i_1(t)\rangle|_{T_s} &= d(t)\left[\langle i_{L1}(t)\rangle|_{T_s} + \langle i_{L2}(t)\rangle|_{T_s}\right] \\
\langle u_2(t)\rangle|_{T_s} &= d(t)\left[\langle u_{C1}(t)\rangle|_{T_s} + \langle u_{C2}(t)\rangle|_{T_s}\right] \\
\langle i_2(t)\rangle|_{T_s} &= [1-d(t)]\left[\langle i_{L1}(t)\rangle|_{T_s} + \langle i_{L2}(t)\rangle|_{T_s}\right]
\end{aligned} \tag{1}$$

where the averaged value is denoted by $\langle\square\rangle\big|_{T_S}$ and $d(t)$ is a duty cycle as a control input. We have selected $\langle i_1(t)\rangle\big|_{T_S}$ and $\langle u_2(t)\rangle\big|_{T_S}$ as the switch network independent inputs, $\langle i_2(t)\rangle\big|_{T_S}$ and $\langle u_1(t)\rangle\big|_{T_S}$ are switch network dependent outputs. By elimination of the converter's signals $\langle u_{C1}(t)\rangle\big|_{T_S}$, $\langle u_{C2}(t)\rangle\big|_{T_S}$, $\langle i_{L1}(t)\rangle\big|_{T_S}$ and $\langle i_{L2}(t)\rangle\big|_{T_S}$ equation (1) can be rearranged in a form where the switch dependent outputs are expressed as a function of switch independent inputs and duty cycle $d(t)$:

$$\begin{aligned}\langle u_1(t)\rangle\big|_{T_s} &= \frac{1-d(t)}{d(t)}\langle u_2(t)\rangle\big|_{T_s}\\ \langle i_2(t)\rangle\big|_{T_s} &= \frac{1-d(t)}{d(t)}\langle i_1(t)\rangle\big|_{T_s}.\end{aligned} \tag{2}$$

Equation (2) describes the averaged model of the switch network that is valid for the frequencies sufficiently less than the switching frequency. By perturbation and linearization of (2) we can construct a small-signal ac model:

$$\begin{aligned} d(t) &= D+\tilde{d}\\ \langle u_1(t)\rangle\big|_{T_s} &= U_1+\tilde{u}_1(t)\\ \langle i_1(t)\rangle\big|_{T_s} &= I_1+\tilde{i}_1(t)\\ \langle u_2(t)\rangle\big|_{T_s} &= U_2+\tilde{u}_2(t)\\ \langle i_2(t)\rangle\big|_{T_s} &= I_2+\tilde{i}_2(t).\end{aligned} \tag{3}$$

With the substitution of (3) into (2) and by assumption that the nonlinear terms $\tilde{d}(t)\tilde{u}_1(t)$ and $\tilde{d}(t)\tilde{u}_2(t)$ can be neglected, the following is obtained:

$$\begin{aligned}(U_1+\tilde{u}_1) &= \frac{(1-D)}{D}(U_2+\tilde{u}_2)-\tilde{d}\frac{U_1}{D(1-D)}\\ (I_2+\tilde{i}_2) &= \frac{(1-D)}{D}(I_1+\tilde{i}_1)-\tilde{d}\frac{I_2}{D(1-D)}\end{aligned} \tag{4}$$

where the last term in both lines is driven by the control input $\tilde{d}$ and can be represented by an independent voltage or current source. Equation (4) describes the averaged switch network model that contains both dc and small-signal ac terms. It also shows that the switch network performs the function of the transformation of dc and small-signal ac voltage and current levels according to the $(1-D)/D$ conversion ratio and also initiates ac voltage and current variations into the converter circuit driven by the control input $\tilde{d}$. In Figure 4 the averaged model of switch network in the SEPIC converter is shown.

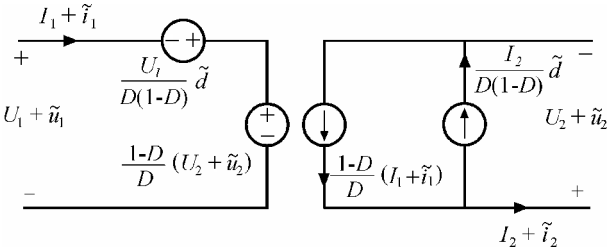

Fig. 4 Averaged model of the switch network in the nonisolated SEPIC converter

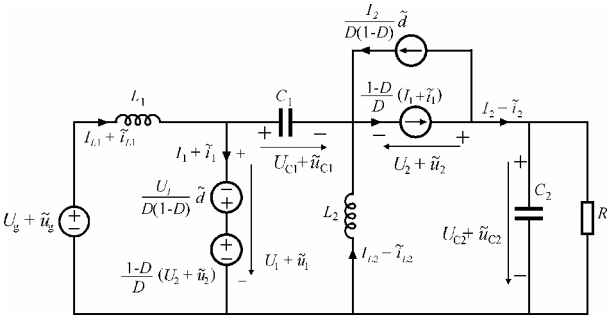

Fig. 5 Averaged circuit topology of the nonisolated SEPIC converter

When this averaged model is inserted into the SEPIC circuit topology of Figure 2, the dc and small-signal ac SEPIC model, shown in Figure 5, is obtained.

By applying the first and second Kirchoff's laws on the averaged circuit topology the full order state-space dynamic model of the SEPIC converter can be obtain:

$$\begin{aligned}\frac{d\left(I_{L1}+\tilde{i}_{L1}\right)}{dt} &= \frac{D-1}{L_1}(U_{C1}+\tilde{u}_{C1})+\frac{D-1}{L_1}(U_{C2}+\tilde{u}_{C2})+\frac{1}{L_1}\left(U_g+\tilde{u}_g\right)+\frac{U_1}{L_1(1-D)}\tilde{d}\\ \frac{d\left(I_{L2}+\tilde{i}_{L2}\right)}{dt} &= \frac{D}{L_2}(U_{C1}+\tilde{u}_{C1})-\frac{1-D}{L_2}(U_{C2}+\tilde{u}_{C2})+\frac{U_1}{L_2(1-D)}\cdot\tilde{d}\\ \frac{d(U_{C1}+\tilde{u}_{C1})}{dt} &= \frac{1-D}{C_1}\left(I_{L1}+\tilde{i}_{L1}\right)-\frac{D}{C_1}\left(I_{L2}+\tilde{i}_{L2}\right)-\frac{1}{1-D}\cdot\frac{U_{C2}}{RC_1}\cdot\tilde{d}\\ \frac{d(U_{C2}+\tilde{u}_{C2})}{dt} &= \frac{1-D}{C_2}\left(I_{L1}+\tilde{i}_{L1}\right)+\frac{1-D}{C_2}\left(I_{L2}+\tilde{i}_{L2}\right)-\frac{1}{RC_2}(U_{C2}+\tilde{u}_{C2})-\frac{1}{1-D}\frac{U_{C2}}{RC_2}\tilde{d}.\end{aligned} \tag{5}$$

From (5) the control-to-output transfer function can be written by setting the input voltage variation $\tilde{u}_g$ to zero and line-to-output transfer function by setting the duty cycle variation $\tilde{d}$ to zero:

$$\frac{\tilde{u}_{C2}(s)}{\tilde{d}(s)} = \frac{a_3 s^3 + a_2 s^2 + a_1 s + a_0}{s^4 + b_3 s^3 + b_2 s^2 + b_1 s + b_0}$$
$$\frac{\tilde{u}_{C2}(s)}{\tilde{u}_g(s)} = \frac{a_2 s^2 + a_0}{s^4 + b_3 s^3 + b_2 s^2 + b_1 s + b_0} \quad (6)$$

where the corresponding parameters of the nominators and denominators are:

$$a_0 = \frac{U_g}{C_1 C_2 L_1 L_2}, \quad a_1 = -\frac{U_{C2} D}{(1-D) R C_1 C_2 L_2},$$
$$a_2 = \frac{U_g (L_1 + L_2)}{C_2 L_1 L_2}, \quad a_3 = -\frac{U_{C2}}{(1-D) R C_2},$$
$$b_0 = \frac{(1-D)^2}{C_1 C_2 L_1 L_2}, \quad b_1 = \frac{1}{R C_1 C_2}\left(\frac{(1-D)^2}{L_1} + \frac{D^2}{L_2}\right),$$
$$b_2 = \frac{(1-D)^2 (C_2 L_2 + C_1 L_2 + C_1 L_1) + D^2 C_2 L_1}{C_1 C_2 L_1 L_2},$$
$$b_3 = \frac{1}{R C_2}.$$

The design of the converter voltage controller is based on the control-to-input transfer function $\tilde{u}_{C2}(s)/\tilde{d}(s)$. Its Bode plot is calculated by MATLAB software package [7] and shown in Figure 6. From the plot can be observed that the system is of the 4-th order and it has two resonant frequencies.

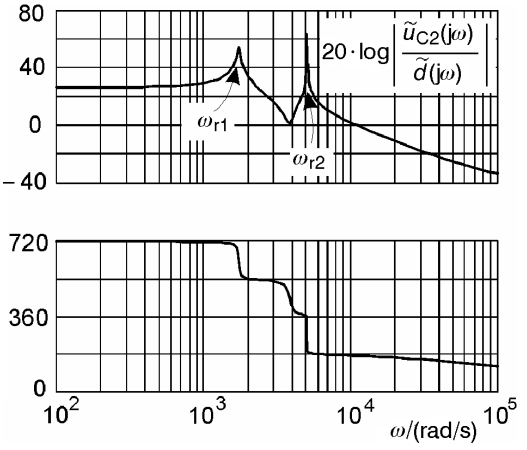

Fig. 6 Bode plot of $\tilde{u}_{C2}(s)/\tilde{d}(s)$ for the nonisolated SEPIC converter

3 CIRCUIT AVERAGING AND AVERAGED SWITCH MODELING FOR ISOLATED SEPIC CONVERTER

When the second inductor L_2 in the SEPIC converter topology is realized using two windings, as shown in Figure 7, we get the isolated version of the converter. The ideal transformer provides isolation and a turn ratio while its magnetizing inductance equals L_2 and performs the energy-storage function.

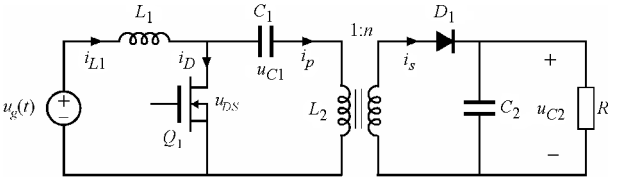

Fig. 7 The isolated SEPIC converter circuit topology

By introduction of the transformer into the circuit topology the circumstances on the switch network are changed as shown in Figure 8. When the transistor is switched on, the magnetizing current flows through the primary winding and the secondary winding current is zero. When the transistor is switched off and diode is conducting, the magnetizing current flows through the secondary winding to the load. Additionally, the input current i_{L1} flows through the primary winding and induces an additional component of the secondary current i_{L1}/n, which also flows to the load.

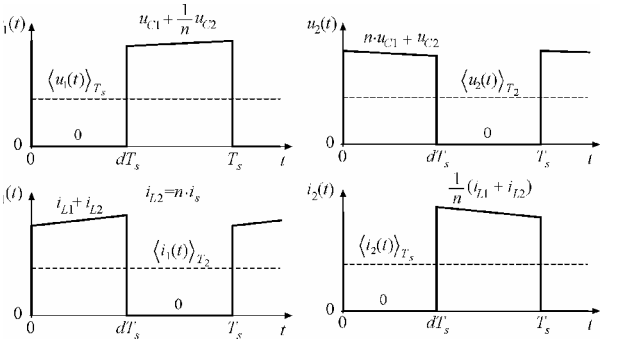

Fig. 8 The isolated SEPIC switch network terminal waveforms

Considering these new circumstances in (1), (2) and (3) the model of the averaged isolated SEPIC switch network can be obtained as:

$$(U_1 + \tilde{u}_1) = \frac{(1-D)}{n \cdot D}(U_2 + \tilde{u}_2) - \tilde{d}\frac{U_1}{D(1-D)}$$
$$(I_2 + \tilde{i}_2) = \frac{(1-D)}{n \cdot D}(I_1 + \tilde{i}_1) - \tilde{d}\frac{I_2}{D(1-D)}. \quad (7)$$

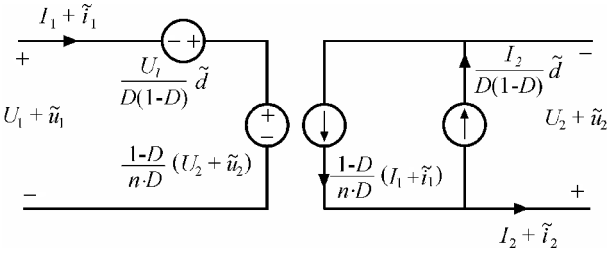

Fig. 9 Averaged model of the switch network in the isolated SEPIC converter

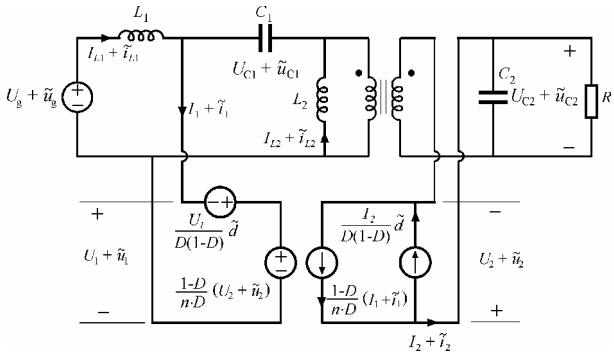

Fig. 10 Averaged circuit topology of the isolated SEPIC converter

Comparison between (7) and (4) shows that only conversion ratio of the transformation of dc and small-signal ac voltage and current levels change from (1–*D*)/*D* to (1–*D*)/*nD*. In Figure 9 the averaged model of switch network in the SEPIC converter is shown.

By inserting the averaged model of switch network into the isolated SEPIC converter circuit topology we obtain the dc and small-signal ac isolated SEPIC model, shown in Figure 10.

As in the previous case the application of the first and second Kirchoff's laws leads to the full order dynamic model of the isolated SEPIC converter in state space:

$$
\begin{aligned}
\frac{d(I_{L1}+\tilde{i}_{L1})}{dt} &= -\frac{1-D}{L_1}(U_{C1}+\tilde{u}_{C1}) - \frac{1-D}{nL_1}(U_{C2}+\tilde{u}_{C2}) + \frac{U_1}{L_1(1-D)}\tilde{d} + \frac{1}{L_1}(U_g+\tilde{u}_g)\\
\frac{d(I_{L2}+\tilde{i}_{L2})}{dt} &= \frac{D}{L_2}(U_{C1}+\tilde{u}_{C1}) - \frac{1-D}{nL_2}(U_{C2}+\tilde{u}_{C2}) + \frac{U_1}{L_2(1-D)}\cdot\tilde{d}\\
\frac{d(U_{C1}+\tilde{u}_{C1})}{dt} &= \frac{1-D}{C_1}(I_{L1}+\tilde{i}_{L1}) - \frac{D}{C_1}(I_{L2}+\tilde{i}_{L2}) - \frac{n}{1-D}\cdot\frac{U_{C2}}{RC_1}\cdot\tilde{d}\\
\frac{d(U_{C2}+\tilde{u}_{C2})}{dt} &= \frac{1-D}{nC_2}(I_{L1}+\tilde{i}_{L1}) + \frac{1-D}{nC_2}(I_{L2}+\tilde{i}_{L2}) - \frac{1}{RC_2}(U_{C2}+\tilde{u}_{C2}) - \frac{1}{1-D}\frac{U_{C2}}{RC_2}\tilde{d}.
\end{aligned}
\tag{8}
$$

From (8) the control-to-output transfer function can be found by setting the input voltage variation $\tilde{u}_g$ to zero and applying the Laplace's transform:

$$
\frac{\tilde{u}_{C2}}{\tilde{d}(s)} = \frac{N_o(s)}{D_E(s)} = \\
= \frac{a_{i3}s^3 + a_{i2}s^2 + a_{i1}s + a_{i0}}{s^4 + b_{i3}s^3 + b_{i2}s^2 + b_{i1}s + b_{i0}} \tag{9}
$$

where the nominator $N_o(s)$ and denominator $D_E(s)$ coefficients are:

$$
a_{i0} = \frac{U_g}{nC_1C_2L_1L_2}, \qquad a_{i1} = -\frac{U_{C2}D}{(1-D)RC_1C_2L_2},
$$

$$
a_{i2} = \frac{U_g(L_1+L_2)}{nC_2L_1L_2}, \qquad a_{i3} = -\frac{U_{C2}}{(1-D)RC_2},
$$

$$
b_{i0} = \frac{(1-D)^2}{n^2C_1C_2L_1L_2}, \qquad b_{i1} = \frac{1}{RC_1C_2}\left(\frac{(1-D)^2}{L_1} + \frac{D^2}{L_2}\right),
$$

$$
b_{i2} = \frac{(1-D)^2(n^2C_2L_2 + C_1L_2 + C_1L_1) + D^2n^2C_2L_1}{n^2C_1C_2L_1L_2},
$$

$$
b_{i3} = \frac{1}{RC_2}.
$$

The Bode plots of control to input transfer function $\tilde{u}_{C2}(s)/\tilde{d}(s)$ for different values of duty cycle *D* and turn ratio *n* are shown in Figures 11a,b. In Figure 11a it can be observed how the Bode plots and resonant frequencies depend on different turn ratios. For the higher turn ratio *n* the first resonant frequency is lower. In the second case (Figure 11b) we can observed how the different duty cycles at the fixed turn ratio *n* = 2 influence on resonant frequencies. For the higher duty cycles *D* the first resonant frequency is lower and more separated from the second one. This could be a very impor-

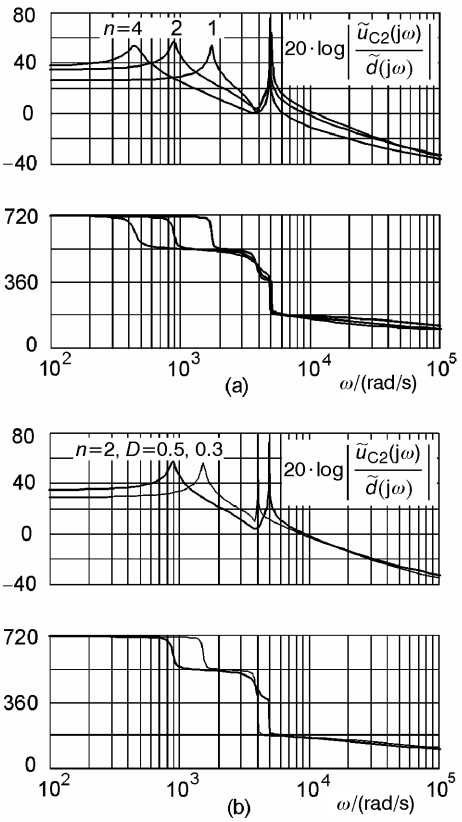

Fig. 11 Bode plot of $\tilde{u}_{iC2}(s)/\tilde{d}_i(s)$ for the isolated SEPIC converter at different turn ratios n and duty cycles D

tant issue in design-oriented analysis in which the SEPIC converter parameter values such as turn ratio and duty cycle for the nominal operating point are chosen to meet the specifications and design goals.

4 ISOLATED SEPIC CONVERTER DYNAMIC MODEL VERIFICATION

Verification of the derived dynamic model of the isolated SEPIC converter was done by MATLAB software package using SimPowerSystems toolbox that works together with SIMULINK to model electrical, mechanical and control systems. The switching elements were modelled with adequate snubber circuit while the transformer, inductances and capacitors were modelled as ideal elements with the following values $L_1 = 1.2$ mH, $L_2 =$ $= 1$ mH, $C_1 = 22$ μF, $C_2 = 390$ μF, $R = 0.9$ Ω and turn ratio $n = 0.16$. The simulations were performed by variable-step and integration method ode23tb(stiff/TR-BDF2).

In Figure 12 the transient responses of the full order dynamic model of the SEPIC converter and

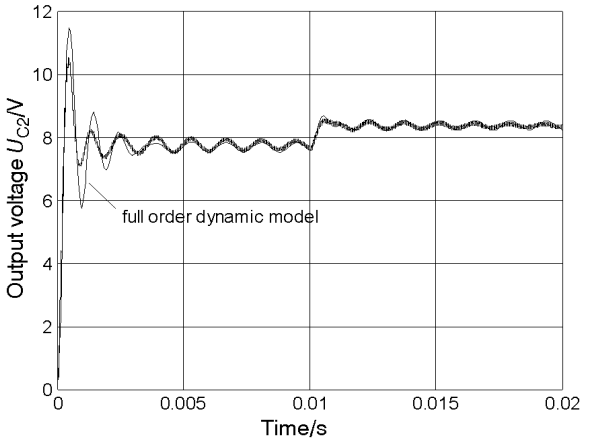

Fig. 12 Transient responses obtained by simulation of the full order dynamic model in SimPowerSystems at D = 0.5

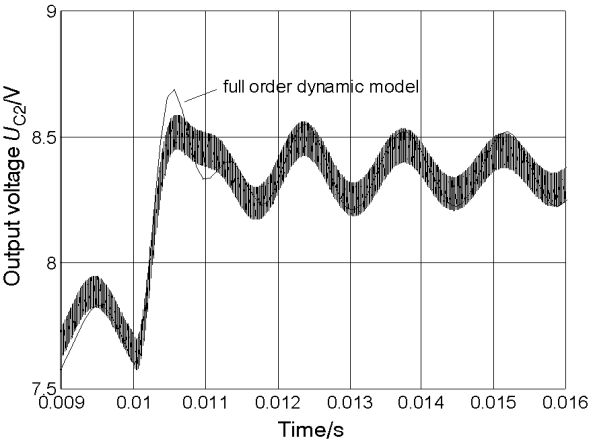

Fig. 13 Transient responses of the full order dynamic model (zoom in) at the step change of duty cycle for 2 % at t = 0.01 s

converter simulation in SimPowerSystems for the step change of duty cycle $D = 0.5$ at $t = 0$ s and for 2 % ($D = 0.52$) at $t = 0.01$ s can be observed. From Figure 13 where the transient responses are zoomed in for the small change of duty cycle is evident that the both traces matched almost perfect.

The obtained results of the full order dynamic model of the SEPIC converter were compared with the results of the reduced (second) order dynamic model derived by injected current method [3, 4] and given by:

$$\frac{\tilde{u}_{C2}(s)}{\tilde{d}(s)} = G_R \frac{-a_{ro1}s + 1}{b_{ro2}s^2 + b_{ro1}s + b_{ro0}} \qquad (10)$$

where the coefficients of the control to input transfer function are given by:

$$M = \frac{nD}{1-D}, \quad G_R = \frac{U_g (n+M)^2}{n},$$

$$a_{ro1} = \left(M^2 - \frac{2n+M}{n+M} \cdot \frac{RT_s}{2L_1} \right) \frac{L_1}{R},$$

$$b_{ro2} = (n+M)^2 C_2 L_1, \quad b_{ro1} = \left((n+M)^2 + \frac{RT_s}{2L_1} \right) \frac{L_2}{R}.$$

The same test as for the full order dynamic model was also performed for the reduced order dynamic model (10). The results are shown in Figure 14 and Figure 15. They confirm that the reduced order dynamic model eliminates the second resonant frequency (Figure 6 and Figure 11). Therefore its transient response doesn't match completely by the transient response of the converter simulation in SimPowerSystems. For both cases the average value of the converter output voltage is the same in steady state.

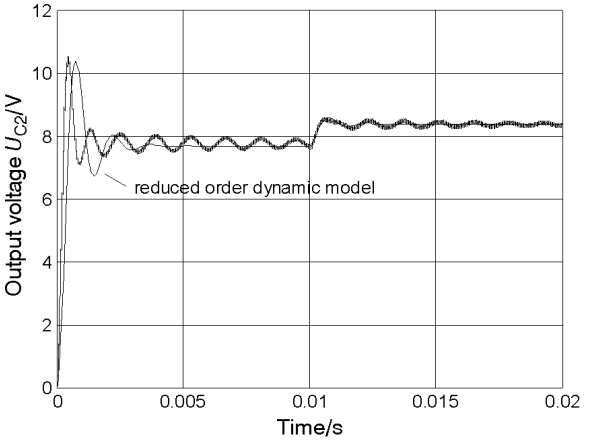

Fig. 14 Transient responses obtained by simulation of the second order dynamic model in SimPowerSystems at D = 0.5

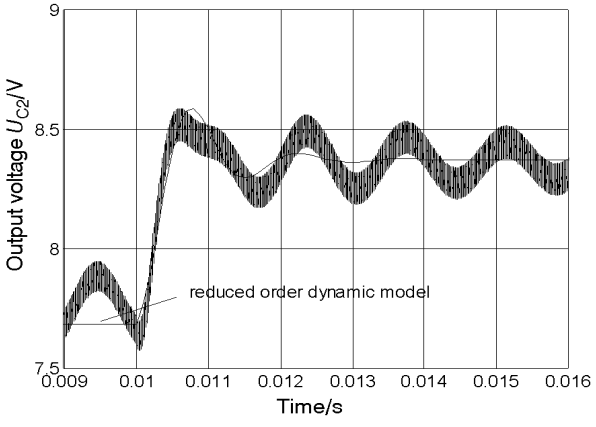

Fig. 15 Transient responses of the second order dynamic model (zoom in) at the step change of duty cycle for 2 % at t = = 0.01 s

5 DESIGN GUIDELINES FOR ISOLATED SEPIC CONVERTER

If the fourth order SEPIC converter is properly designed, its denominator $D_E(s)$ consists of two quadratic factors whose resonances should be well separated and almost entirely damped by the load. The resonant frequencies are not significantly affected by parasitic resistances under normal loading conditions. Therefore we can write:

$$D_E(s) = (s^2 + 2D_1\omega_{01}s + \omega_{01}^2)(s^2 + 2D_2\omega_{02}s + \omega_{02}^2) = \\ = s^4 + b_{r3}s^3 + b_{r2}s^2 + b_{r1}s + b_{r0} \tag{11}$$

When we assume that the system is moderate or low damped and the resonances are well separated ($\omega_{02} \doteq \omega_{01}$) we get:

$$\begin{aligned} b_{r3} &= 2D_1\omega_{01} + 2D_2\omega_{02} \doteq 2D_2\omega_{02} = b_{i3} \\ b_{r2} &= \omega_{01}^2 + \omega_{02}^2 + 4D_1D_2\omega_{01}\omega_{02} \doteq \omega_{02}^2 = b_{i2} \\ b_{r1} &= 2D_1\omega_{01}\omega_{02}^2 + 2D_2\omega_{02}\omega_{01}^2 = b_{i1} \\ b_{r0} &= \omega_{01}^2\omega_{02}^2 = b_{i0}. \end{aligned} \tag{12}$$

Finally we can determinate the resonance frequencies and damping factors as:

$$\omega_{02} \doteq \sqrt{b_{i2}} = \\ = \sqrt{\frac{(1-D)^2(n^2C_2L_2 + C_1L_2 + C_1L_1) + D^2n^2C_2L_1}{n^2C_1C_2L_1L_2}} \tag{13}$$

$$D_2 \doteq \frac{1}{2RC_2\omega_{02}} \tag{14}$$

$$\omega_{01} \doteq \frac{\sqrt{b_{i0}}}{\omega_{02}} = \\ = \frac{(1-D)}{\sqrt{(1-D)^2(n^2C_2L_2 + C_1L_2 + C_1L_1) + D^2n^2C_2L_1}} \tag{15}$$

$$D_1 \doteq \frac{\omega_{01}}{2R}\left[n^2L_2 + \frac{n^2L_1D^2}{(1-D)^2} - \frac{1}{C_2\omega_{02}^2} \right]. \tag{16}$$

The above equations can be used when the transformer turn ratio n and duty cycle D of the SEPIC converter have to be determined.

6 CONCLUSIONS

In this paper the full order dynamic models of the nonisolated and isolated SEPIC converters were derived applying the method of circuit averaging and averaged switch modelling. The models give insight into the physical properties of the converter and relations between converter parameters and dynamic properties of the system. The derived dynamic model for the isolated SEPIC converter was verified by simulation of the SEPIC converter in SimPowerSystems and compared with the reduced order dynamic model. The obtained results show the superiority of the full order dynamic model over the last one. Therefore it presents a good starting point in converter design-oriented analysis as well as in design of the feedback control loop. Furthermore, the full order dynamic model can be easily improved by taking into consideration the series resistance of the inductances.

REFERENCES

[1] R. P. Massey, E. C. Snyder, **High Voltage Single-Ended dc-dc Converter.** PESC'77 Record, pp. 156–159, 1977.

[2] R. D. Middlebrook, S. Cuk, **A General Unified Approach to Modeling Switching Converter Power Stages.** PESC'76 Record, pp. 19–34, 1976.

[3] A. S. Kislovski, R. Ridl, N. O. Socal, **Dynamic Analysis of Switchig Mode dc-dc Converter.** Van Nostrand Reinhold, New York, 1991.

[4] N. Mohan, T. Undeland, W. Robbins, **Power Electronics, Devices, Converter, Application and Design.** John Willey & Sons, New York, Singapore, Toronto, Brisbane, 1989.

[5] V. Vorperian, **Simplified Analysis of PWM Converters Using the Model of the PWM switch: Parts I and II.** IEEE Trans. Aerospace and Electronic Systems 26, pp. 490–505, May 1990.

[6] R. W. Erickson, D. Maksimović, **Fundamentals of Power Electronics, second edition.** Kluwer Academic Publishers, 2001.

[7] ..., **Matlab.** Version 6.5, Release 13, Mathworks, Inc.

Dinamička analiza SEPIC pretvarača. U radu je prikazana dinamička analiza SEPIC pretvarača (engl. **S**ingle **E**nded **P**rimary **I**nductance **C**onverter) bez galvanskog odvajanja i s galvanskim odvajanjem. U analizi se sklopke (tranzistori i diode) nadomještaju ekvivalentnim modelom s usrednjavanjem zasnovanim na širinsko-impulsnoj modulaciji. SEPIC pretvarači omogućuju veliki raspon ulaznog napona pretvarača. Sam pretvarač može raditi kao silazni i uzlazni dc-dc pretvarač. Strukturu pretvarača osim poluvodičkih komponenata čine i dvije zavojnice i dva kondenzatora, što omogućuje njegovo modeliranje diferencijalnom jednadžbom četvrtoga reda. Na dinamiku pretvarača značajan utjecaj imaju i vrijeme vođenja i transformatorski prijenosni. U članku su dane preporuke za projektiranje SEPIC pretvarača kojima se postiže dovoljno veliko razdvajanje rezonantnih frekvencija koje se pojavljuju u frekvencijskoj karakteristici pretvarača. Razvijeni je model pretvarača provjeren simulacijama pomoću programskog alata SimPowerSystems programa MATLAB.

Ključne riječi: SEPIC pretvarač, dinamička analiza, ekvivalentni model s PWM usrednjavanjem

AUTHORS' ADDRESS

Dr. Alenka Hren
e-mail: alenka.hren@uni-mb.si

Prof. dr.Miro Milanovič
e-mail: milanovic@uni-mb.si

University of Maribor
Faculty of Electrical Engineering and Computer Science
Smetanova 17, 2000 Maribor, Slovenia

Received: 2007-10-18